doi: 10.1109/TIE.2015.2509914

Sliding mode analysis of the dynamics of sigma-delta controls of dielectric charging

Manuel Dominguez-Pumar, Sergi Gorreta, Joan Pons-Nin
Micro and Nano Technologies Group, Universitat Politècnica de Catalunya, Barcelona, Spain
corresponding author email: manuel.dominguez@upc.edu

***Abstract*—The purpose of this paper is to show that sigma-delta controllers of dielectric charge can be analyzed using the tools of sliding mode controllers, in the infinite sampling frequency approximation. This allows to study the dynamics of the hidden state variables related to the charge in the dielectric, as well as the reachability and stability of the control method. Furthermore, it is also possible to explain the response of the control bitstream as a function of the dynamical model of the system. This approach not only provides insight into the dynamics of the charge controllers, understood as hybrid systems, it also simplifies the modelling and simulations of the system.**

dielectric charge control, sliding mode control, charge trapping, switched systems, hybrid systems

I. Introduction

Charge trapping in dielectrics is a common problem for a large number of devices, such as in the case of organic field effect transistors, [1], [2], thin film transistors, [3], or in the inter-polysilicon dielectric present in flash memories, [4], [5] where charge trapping and detrapping may generate stress-induced leakage currents. Trapped charge generates a non desired long term drift in the device characteristics. In the case of electrostatically actuated MEMS devices, this phenomenon also represents a reliability problem [6]–[9]. In order to mitigate the generation of charge in dielectrics several open-loop strategies have been proposed in the past [10]. In the long term, though, these techniques do not guarantee the absence of drift in the characteristics of the device. In [11]–[13] different closed-loop methods for the control of total dielectric charge have been proposed and proved with MEMS devices. In particular, the methods proposed in [13] and [14] allow to fix, within some limits, arbitrary levels of total dielectric charge while the generated actuation is that of a first-order and a second-order sigma-delta modulator, respectively.

The purpose of this paper is to analyze the dynamics of the state variables of the dielectric charging kinetic models when the device is being controlled by a sigma-delta control of charge. It will be shown that this dynamics can be analyzed with the tools of sliding mode controllers (SMC). SMCs are ubiquitous to many applications [15], [16]. These nonlinear controllers alter the dynamics of the system by applying a discontinuous control signal so that under some conditions the system 'slides' on a certain control surface. This is generally done in order to obtain a certain wanted behaviour of the system. On the other hand, any dielectric charge control method using a discontinuous control signal, and such that it keeps constant the total dielectric charge, will perform a 'sliding motion' on a surface of the space of state variables. This surface is precisely the one defined by the condition: 'total dielectric charge constant'. This means that any control method guaranteeing a constant total dielectric charge will generate a sequence of actuation voltages that can be analyzed using the tools of sliding mode controllers. This in particular will explain the behaviour of the binary sequences generated by sigma-delta dielectric charge controls.

Sigma-delta dielectric charge controllers periodically monitor the total dielectric charge through an indirect measurement. A binary sequence of actuation waveforms, namely BIT0 and BIT1 symbols, is then applied to the device to reach and keep the desired level of charge. In an initial phase, the control applies only one of the symbols, increasing or decreasing the charge until the target charge is reached. In a second phase, once around the desired level of charge, there is a fast switching between symbols in the actuation sequence to keep charge around this desired level. We analyze the dynamics during this second phase using the tools of sliding mode control. The average actuation bitstream generated by these control schemes will be seen as the equivalent control, in the Filippov sense, of a sliding regime. This interpretation will allow to understand the hidden dynamics of the state variables related to the multiexponential models of the dielectric charge. In particular it will be possible to explain the slow-time variation of the control bitstream usually obtained in the measurements.

The analysis will be carried out using the concept of an 'average system', [17], [18]. With this approach the continuous switching produced by the actuation symbols will be approximated by an average system, under the infinite sampling frequency approximation. In a second step, the rapid switching produced by the sigma-delta controllers is equivalent to the fast switching produced in relay feedback systems, or the slide regime in sliding mode controllers. This approach is new to all previously published papers on dielectric charge control based on sigma-delta modulators.

The dynamics of the charge state variables depends on the instantaneous voltage applied. Since in sigma-delta controls of dielectric charge only two voltages are applied, these systems fall into the category of switched affine systems: $\dot{x} = A_{\sigma(t)}x + B_{\sigma(t)}$ for a switching signal $\sigma \in \{b_0, b_1\}$ that will depend on the state vector x, and where $\{A_{b_0}, B_{b_0}\}$and

Figure 1. Sigma-delta control of dielectric charging: a) First order, b) Second order.

$\{A_{b_1}, B_{b_1}\}$ are the average systems associated with each actuation symbol, BIT0 and BIT1 respectively. It will be assumed that matrices A_{b_i} share a common Lyapunov solution.

All the experimental results presented in this paper have been obtained with MEMS fabricated with PolyMUMPS technology. The measurements have been made in the contactless case (actuation voltages below pull-in voltage).

Section II briefly explains the first and second order sigma-delta control methods, the multiexponential charging models and the average actuation obtained with the BIT0 and BIT1 waveforms. The reachability conditions of the control surface are analyzed in Section III. Section IV presents the dynamics within the sliding region on the control surface. Finally, in Section V the comparison between the analytical results from this work and experimental measurements is made using the devices and charging models of [19].

II. Sigma-Delta control of dielectric charging

The structure of the sigma-delta controls of dielectric charging can be seen in Figure 1. The purpose of these controls is to enforce a net quantity of dielectric charge in the device, Q_d. Changes in the net dielectric charge displace horizontally the C-V curves of the device. Other phenomena, such as environmental factors: temperature, etc., together with charge inhomogeneity, generate vertical displacements of the C-V curve, [13]. The net amount of charge in the dielectric is inferred by measuring the capacitance of the device at two voltages (V^+ and V^-) of different sign, within the same sampling period. The differential measurement, namely $\Delta C(t) := C(t, V^+) - C(t, V^-)$ has been shown to be under some conditions an affine function of the total charge in the dielectric, [13]:

$$\Delta C(t) = C(t, V^+) - C(t, V^-) = \alpha[(V^+)^2 - (V^-)^2] - 2\alpha V_{\text{sh}}(t)[V^+ - V^-] \quad (1)$$

where α is the second order coefficient of the parabolic approximation of the C-V curve, and $V_{\text{sh}}(t) = Q(t)/C_d$, with C_d being the capacitance of the dielectric layer. This means that for each sampling time, an indirect measurement of the total amount of charge is made. In the case of using the symbols of Figure 2, the capacitance measurements are made at times $(1-\delta)T_S$ and T_S.

The proposed controls generate an actuation given by a sequence of BIT0 and BIT1 symbols. In the case of a first-order control the actuation will depend on whether the sampled charge is either above or below the desired level, $b_n = \text{sgn}(Q_n - Q_{\text{target}})$ (Fig. 1.a), where Q_n is the instantaneous total charge at time nT_S. In the second order case, there is an additional numerical integrator that allows to generate a second order noise shaping of the bitstream (Fig. 1.b).

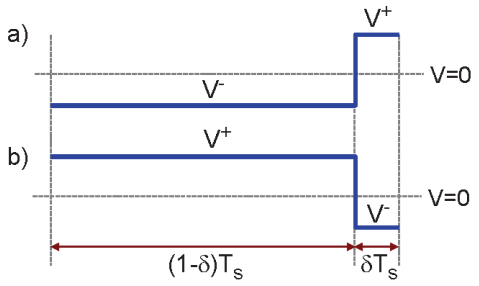

Figure 2. Bipolar voltage symbols used to actuate the MEMS. BIT0 (a) applies a constant voltage V^- for a time $(1-\delta)T_S$, followed by V^+ for a short time δT_S. In BIT1 (b), V^+ is applied during $(1-\delta)T_S$, then V^- for δT_S. T_S is the sampling period of the sigma-delta control.

In both cases, the dielectric acts as a leaky integrator: it is a charge reservoir. There are two competing charge contributions: the charge continuously being leaked out of the dielectric and the charge being injected by the actuation. Once a certain Q_{target} level is fixed, the adequate actuation will be generated to account for the losses in the dielectric at this total target charge level.

A. Multiexponential time-varying charge model

The objective of this section is to present the multiexponential time-varying model so that it can be analyzed within the context of sliding mode control. In the contactless case and assuming a multiexponential model, [11]–[13], the response to a voltage step of the positive, $q^p(t)$, and negative, $q^n(t)$, charge in the dielectric in a previously discharged device is:

$$q^p(t) = \begin{cases} Q^p_{\text{max}} \sum_i \zeta_i^p e^{-t/\tau^p_{Di}} & V > 0 \\ Q^p_{\text{max}}(1 - \sum_i \zeta_i^p e^{-t/\tau^p_{Ci}}) & V < 0 \end{cases} \quad (2)$$

$$q^n(t) = \begin{cases} Q^n_{\text{max}}(1 - \sum_i \zeta_i^n e^{-t/\tau^n_{Ci}}) & V > 0 \\ Q^n_{\text{max}} \sum_i \zeta_i^n e^{-t/\tau^n_{Di}} & V < 0 \end{cases} \quad (3)$$

The charge and discharge time constants for each charge sign component are, respectively, τ_{Ci} and τ_{Di}. Q^n_{max} and Q^p_{max} are the maximum values of negative and positive charge, respectively, and the coefficients ζ_i specify how these total charges are distributed among the state variables, and therefore we have $\sum_i \zeta_i^n = \sum_i \zeta_i^p = 1$ and $0 \le \zeta_i^n, \zeta_i^p \le 1$. The maximum amount of charge of each exponential is then defined as $Q^{p,i}_{\text{max}} = Q^p_{\text{max}}\zeta_i^p$ and $Q^{n,i}_{\text{max}} = Q^n_{\text{max}}\zeta_i^n$.

It must be noted that in the above equations there is an implicit nonlinear dependence of the time parameters (time constants and amplitudes) on the applied voltages. The above equations, in the exact form of (2) and (3), are valid for an initially discharged device on which either a constant positive, or negative, voltage is applied. In order to analyze the time

evolution of the system for an arbitrary voltage signal taking only two voltage values, i.e., $v(t) \in \{V^+, V^-\}$, we describe the time-varying linear system as:

$$\begin{aligned} \dot{x}(t) &= A_1 x(t) + B_1, \qquad v(t) = V^+ \\ \dot{x}(t) &= A_0 x(t) + B_0, \qquad v(t) = V^- \end{aligned} \tag{4}$$

where $A_i \in \mathbb{R}^{n\times n}$, $B_i \in \mathbb{R}^n, i = \{0, 1\}$, and $v(t) \in \mathbb{R}$ is the control voltage applied to the device: either a constant positive or negative voltage: $V^+ > 0$, or $V^- < 0$. In the contactless case, we may use one of the charging models obtained in [19]. The parameters of this model are summarized in table I. The maximum charge in the dielectric, Q_{max}, and the maximum voltage shift in the C-V curve are related by the capacitance of the dielectric layer, C_d: $V_{\text{sh}}^{\text{max}} = Q_{\text{max}}/C_d$. With this model, we have that for a positive charge component, $B_0^i = Q_{\text{max}}^p \zeta_i^p / \tau_i^p, B_1^i = 0$; whereas $B_1^j = Q_{\text{max}}^n \zeta_j^n / \tau_j^n, B_0^j = 0$ for a negative charge component. This means that $B_0 \geq 0$ and $B_1 \leq 0$. In the contactless case then, for positive voltage we inject negative charge, and positive charge otherwise.

Table I
PARAMETERS FOR THE NEGATIVE AND POSITIVE COMPONENTS OF THE TWO-EXPONENTIAL CHARGE DYNAMICS MODEL, [19].

Parameter	n	p
Q_{max}/C_d [V]	-5.3	5.3
$\tau_{C,1}$ [min]	13	113
$\tau_{C,2}$ [min]	509	2369
$\tau_{D,1}$ [min]	11	87
$\tau_{D,2}$ [min]	483	5567
ζ_1	0.68	0.94
ζ_2	0.32	0.06

At the moment of switching between voltages the state vector, namely $x(t)$, is continuous. The output of the system in our case is the total amount of charge in the dielectric, i.e. $q(t) = q_p(t) + q_n(t)$. This can be seen as a particular case of the usual expression for the output signals of a linear SISO system:

$$q(t) = c^T x(t) \tag{5}$$

where $c = (1, \cdots, 1)^T \in \mathbb{R}^n$ and $q(t) \in \mathbb{R}$ represents the net charge in the device.

B. Description of the actuation waveforms

As commented above, the net charge present in the dielectric can only be measured indirectly. In this regard, the 'quasi-differential' capacitance measurement proposed in [13], is used to make an indirect measurement of the charge at each sampling period by applying two possible waveforms, one on which most of the time a positive voltage is applied, namely BIT1, and another on which most of the time a negative voltage is applied, BIT0 (see Figure 2).

We define the following waveforms:

$$\begin{cases} v_{\text{bit0}}(t) = V^-, & t \in [0, (1-\delta)T_S) \\ v_{\text{bit0}}(t) = V^+, & t \in [(1-\delta)T_S, T_S) \\ v_{\text{bit0}}(t) = 0, & t \notin [0, T_S) \end{cases} \tag{6}$$

and

$$\begin{cases} v_{\text{bit1}}(t) = V^+, & t \in [0, (1-\delta)T_S) \\ v_{\text{bit1}}(t) = V^-, & t \in [(1-\delta)T_S, T_S) \\ v_{\text{bit1}}(t) = 0, & t \notin [0, T_S) \end{cases} \tag{7}$$

With the above definitions, a first-order sigma-delta control of charge is then:

$$\begin{aligned} \dot{x}(t) &= A_{v(t)} x(t) + B_{v(t)} \\ v(t) &= \textstyle\sum_n \frac{1}{2}(1 + b_n) v_{\text{bit1}}(t - nT_S) + \\ &\quad + \frac{1}{2}(1 - b_n) v_{\text{bit0}}(t - nT_S) \\ b_n &= \text{sgn}(c^T x(nT_S) - Q_{\text{target}}) \end{aligned} \tag{8}$$

where $A_{v(t)} = A_1, B_{v(t)} = B_1$ for $v(t) = V^+$; and $A_{v(t)} = A_0, B_{v(t)} = B_0$, for $v(t) = V^-$. This system description is valid in the case of a device described by a multiexponential charging model and actuated by two voltages (V^+ or V^-).

C. Average system: switching within symbols BIT0 and BIT1

The system described in (8) is a time varying linear system whose time variation depends on the actuation voltage, i.e., it is a switched system. The switching in the actuation voltage for each applied symbol (BIT0 or BIT1) is required to have an indirect measurement of the instantaneous net dielectric charge. In the usual implementations of these controls the sampling period is shorter than the smallest time constant of the dielectric charging model. Under an infinite sampling approximation, we may see that that applying a constant sequence of BIT0, or BIT1, symbols is equivalent to having an 'average system' on which this continuous switching is no longer present.

Given a finite set of affine subsystems: $\dot{x}_i = A_i x + B_i, i \in [0, \cdots, n]$, an 'average system' is defined as a convex combination of these subsystems, [17], [18]:

$$\dot{x}_{\text{eq}} = A_{\text{eq}} x + B_{\text{eq}} \tag{9}$$

where $A_{\text{eq}} = \sum_i \alpha_i A_i$, $B_{\text{eq}} = \sum_i \alpha_i B_i$, and $0 < \alpha_i < 1, \sum_i \alpha_i = 1$. This equivalent system can be implemented using a time average control strategy: a switching signal ensures that the dwelling times on each subsystem is proportional to coefficients of the convex combination. Switching must be fast enough so that the largest dwelling time is shorter by at least one order of magnitude than the shortest time constant of all subsystems. This is precisely the situation on which the sigma-delta controls of charge are used.

The deconvolution of multiexponential systems is a notoriously ill-conditioned problem. This means that an infinite number of multiexponential models will always be arbitrarily close to any set of experimental data. On the other hand, it is

known that arbitrary switching of linear systems (even stable ones) can generate unstability. Since unstable behaviour is not observed in dielectric charge experiments, we will add an assumption to the affine models describing the dielectric charge kinetics under the actuation voltages used in the control loop.

Assumption 1: Matrices A_0 and A_1 in (4) possess a common Lyapunov solution.

Not taking into account this restriction, or a similar one, would generate models that would not be coherent since they would be unstable for some sequences of actuation voltages. They would present numerical instabilities and would not be able to predict the behaviour of the system under arbitrary switching of the actuation voltages.

This in particular will guarantee the applicability of the concept 'average system' to the charge models used in this work. Under this assumption, all matrices in the convex cone of matrices A_0 and A_1, $\text{conv}(A_0, A_1)$, have the same Lyapunov solution and are not singular, [20]. Furthermore, the switched linear system $\dot{x} = A_{p(t)}x$, where $p(t)$ is any arbitrary switching signal, is globally exponentially stable. In this manner, instabilities that can arise in linear switchings, even when having Hurwitz matrices [21] [22, p.95], are avoided.

The charging models used in [13], [19] that will be used here obey assumption 1. Now, we may state that:

Proposition 1: The average charge control system of a first-order sigma-delta control of charge, for $T_S \to 0$, is:

$$\dot{x} = \begin{cases} A_{b_1}x + B_{b_1}, & \sigma > 0 \\ A_{b_0}x + B_{b_0}, & \sigma < 0 \end{cases} \tag{10}$$

with $\sigma = c^T x(t) - Q_{\text{target}}$ and where:

$$\begin{array}{rcl} A_{b_1} & = & (1-\delta)A_1 + \delta A_0 \\ B_{b_1} & = & (1-\delta)B_1 + \delta B_0 \\ A_{b_0} & = & \delta A_1 + (1-\delta)A_0 \\ B_{b_0} & = & \delta B_1 + (1-\delta)B_0 \end{array} \tag{11}$$

Proof. The actuation signal, $v(t)$, for a given sampling frequency can be expressed as:

$$\begin{aligned} v(t) = \sum_n \left(\frac{1}{2}(1+b_n)V^+ + \frac{1}{2}(1-b_n)V^-\right) \cdot \\ \mathbf{1}_{[t_n, t_n+(1-\delta)T_S)}(t) + \\ + \left(\frac{1}{2}(1+b_n)V^- + \frac{1}{2}(1-b_n)V^+\right) \cdot \\ \mathbf{1}_{[t_n+(1-\delta)T_S, t_n+T_S)}(t) \end{aligned} \tag{12}$$

with $t_n = nT_S$. Then, applying a technique similar to the one used in [17], we have that:

$$\begin{aligned} x(t_n+T_S) - x(t_n) = \\ = \int_{t_n}^{t_n+T_S} \left[A_{v(\tau)}x(\tau) + B_{v(\tau)}\right] d\tau = \\ \int_{t_n}^{t_n+(1-\delta)T_S} 1/2\left[(1+b_n)A_1 + (1-b_n)A_0\right]x(d\tau)d\tau + \\ \int_{t_n+(1-\delta)T_S}^{t_n+T_S} 1/2\left[(1+b_n)A_0 + (1-b_n)A_1\right]x(d\tau)d\tau + \\ \int_{t_n}^{t_n+(1-\delta)T_S} 1/2\left[(1+b_n)B_1 + (1-b_n)B_0\right]d\tau + \\ \int_{t_n+(1-\delta)T_S}^{t_n+T_S} 1/2\left[(1+b_n)B_0 + (1-b_n)B_1\right]d\tau \end{aligned} \tag{13}$$

It must be noted that in the previous expression no approximation has yet been made. Now, for $T_S \to 0$ and taking into account that x is continuous:

$$\begin{aligned} \frac{1}{T_S}\left(x(t_n+T_S) - x(t_n)\right) \approx \\ (1-\delta)/2\left[(1+b_n)A_1 + (1-b_n)A_0\right]x(t_n) + \\ \delta/2\left[(1+b_n)A_0 + (1-b_n)A_1\right]x(t_n) + \\ (1-\delta)/2\left[(1+b_n)B_1 + (1-b_n)B_0\right] + \\ \delta/2\left[(1+b_n)B_0 + (1-b_n)B_1\right] \end{aligned} \tag{14}$$

Now, calculating the limit $\lim_{T_S \to 0} \frac{x(t_n+T_S)-x(t_n)}{T_S}$, and using the fact that $b_n \to \text{sgn}(\sigma)$, we obtain expressions (10) and (11).

□

The control manifold, $\mathcal{S}$, is the surface $\sigma \equiv 0$. With expressions (10) and (11), it is possible to 'forget' the continuous switching, within each applied bit, necessary to have the indirect measurement of charge. In this way, the dynamics of the system is governed by two average systems, (10), governed by a continuous time switching binary control σ.

III. Reachability conditions of the control surface and existence of a sliding set for the average control system

A. Sufficient reachability conditions of the control surface

The maximum amount of total dielectric charge that the control can set depends on the capability to generate charge trapping and detrapping of the applied voltages, as well as on the value of parameter δ. Once a target dielectric charge is specified (Q_{target}), the control will try to reach this desired charge level. Depending on the affine charging models this level of charge may or may not be reached. The following are sufficient conditions that ensure that the desired level of charge can be reached.

The average system will reach the sliding surface $\sigma(x) = c^T x(t) - Q_{\text{target}} = 0$ in finite time from any initial condition, $x(0)$, if:

$$-c^T A_{b_1}^{-1} B_{b_1} < Q_{\text{target}} \tag{15}$$

and

$$-c^T A_{b_0}^{-1} B_{b_0} > Q_{\text{target}} \tag{16}$$

It follows from the fact that the control hyperplane divides in two parts the state space. On one side of the hyperplane, $\text{sgn}(\sigma) > 0$, the system is described by:

$$\dot{x} = A_{b_1} x + B_{b_1} \tag{17}$$

The above equation simply describes a linear system actuated with a constant control. Therefore we have that:

$$x(t) = e^{A_{b_1} t} x(0) + A_{b_1}^{-1} (e^{A_{b_1} t} - I) B_{b_1}, \qquad t \geq 0 \tag{18}$$

Since the charge model is stable, this means that from any initial $x(0)$ such that $\text{sgn}(c^T x(0) - Q_{\text{target}}) > 0$ the control surface $\sigma = 0$ will be reached if the asymptotic point of this trajectory, $-A_{b_1}^{-1} B_{b_1}$, lies on the other side of the hyperplane, i.e., we have condition (15). A similar analysis can be carried out for the case where the initial condition lies in the region $\text{sgn}(\sigma) < 0$, obtaining condition (16).

This means that if conditions (15) and (16) are fulfilled, the control surface, $\mathcal{S}$, will be continually reached in time (there is no t_0 such that for all $t > t_0$ it is $x(t) \notin \mathcal{S}$). This amounts to not having an asymptotically stable equilibrium point of the system $\dot{x} = A_{b_1} x + B_{b_1}$, (resp. $\dot{x} = A_{b_0} x + B_{b_0}$), inside the set $\sigma > 0$, (resp. $\sigma < 0$).

B. Attractive sliding region within the control surface $\mathcal{S}$

In this section we will apply the techniques used for obtaining fast switches in relay feedback systems that can be found in [23] and [24]. This will provide us with conditions that guarantee the existence of a sliding region within the control surface. First, we have that:

$$\dot{\sigma} = c^T \dot{x} = \begin{cases} c^T (A_{b_1} x + B_{b_1}), & \sigma > 0 \\ c^T (A_{b_0} x + B_{b_0}), & \sigma < 0 \end{cases} \tag{19}$$

We will assume that the control law has been designed to compensate charge, i.e., we have $c^T B_{b_1} < 0$ and $c^T B_{b_0} > 0$. This means that the following subset of the control surface:

$$\begin{aligned} \Omega := \left\{ x \in \mathbb{R}^n : c^T A_{b_1} x < -c^T B_{b_1} \right\} \cap \\ \cap \left\{ x \in \mathbb{R}^n : c^T A_{b_0} x > -c^T B_{b_0} \right\} \cap \mathcal{S} \end{aligned} \tag{20}$$

is attractive. This is due to the fact for any $x \in \mathbb{R}^n$ such that $\sigma(x) < 0$ we will have $\dot{\sigma}(x) > 0$, whereas if $\sigma(x) > 0$ then we will have $\dot{\sigma}(x) < 0$. Therefore we will have $\sigma\dot{\sigma} \leq 0$ in a neighbourhood of Ω. This means that $\Omega \subset \mathcal{S}$, is attractive.

IV. Sliding mode on the control surface

Now, let us assume that the conditions for an attractive control surface are fulfilled. This means that the control surface will be reached and, therefore, $\sigma(x(t)) = c^T x(t) - Q_{\text{target}} = 0$. Now, the average system has been defined as the limit control for infinite sampling frequency and it can be seen as a particular case of:

$$\dot{x}(t) = f(\sigma(x)) \tag{21}$$

Since $f(\sigma(x))$ is a discontinuous function of the state vector, x, the usual results of ordinary differential equations requiring a Lipschitz condition cannot be applied. In these cases, the usual approach consists on obtaining a solution in the sense of Filippov. A solution in the sense of Filippov is obtained when $f(\sigma(x))$ is defined on the sliding surface as a convex linear combination of $f(x^-)$ and $f(x^+)$, understood as the derivative vectors on one side and the other of the discontinuity. This convex combination, $\alpha(x) \in [0, 1]$:

$$\begin{aligned} f(\sigma(x))\Big|_{\sigma(x)=0} := \alpha(x) f(\sigma(\zeta))\Big|_{\zeta \to x, \sigma(\zeta) > 0} + \\ + (1 - \alpha(x))) f(\sigma(\zeta))\Big|_{\zeta \to x, \sigma(\zeta) < 0} \end{aligned} \tag{22}$$

will be such that the derivative will be tangent to the sliding surface, i.e., $f(\sigma(x))\Big|_{\sigma(x)=0} \in T_{x(t)}\mathcal{S}$, with $\mathcal{S}$ being the sliding manifold: $\sigma(x) \equiv 0$.

This last condition in our case implies that the time derivative of $\sigma(x)$, evaluated at any point such that $\sigma(x) = 0$, must be zero:

$$\frac{d}{dt}(\sigma(x))\Big|_{\sigma(x)=0} = 0 = c^T \dot{x} = c^T f(\sigma(x))\Big|_{\sigma(x)=0} \tag{23}$$

where $f(\sigma(x))\Big|_{\sigma(x)=0}$ has been defined in (22), i.e. the system continues to slide on the surface $\sigma(x) = 0$.

Taking this into account we have that $\alpha(x) \in [0, 1]$ must be such that:

$$c^T \left[\alpha(x) \left(A_{b_1} x + B_{b_1} \right) + (1 - \alpha(x)) \left(A_{b_0} x + B_{b_0} \right) \right] = 0 \tag{24}$$

which means that:

$$\alpha(x) = -\frac{c^T A_{b_0} x + c^T B_{b_0}}{c^T (A_{b_1} - A_{b_0}) x + c^T (B_{b_1} - B_{b_0})} \tag{25}$$

Function $\alpha(x)$ provides in fact the average output of the sigma-delta modulator as a function of the instantaneous state vector, $x(t)$. It may also be seen as the equivalent control necessary to keep the system in the sliding surface.

With the expression for $\alpha(x)$ we may now find the nonlinear equation describing the time evolution of the system once it has reached the sliding surface:

$$\dot{x} = \alpha(x) \left(A_{b_1} x + B_{b_1} \right) + (1 - \alpha(x)) \left(A_{b_0} x + B_{b_0} \right) \tag{26}$$

Expressions (25) and (26) define the time evolution of the charge control once it is in the control surface, $\sigma \equiv 0$. This represents the equivalent average system of the systems defined in (10) when the sigma-delta control is in the fast switching regime, the sliding region.

The average bitstream, $\alpha(x)$ is obtained in real applications with a low pass filter (see Figure 1). Although the spectrum

properties of a first order and a second order sigma-delta modulator are clearly different, the average bitstream, i.e., the converted value of both controllers seen now as analog-to-digital converters, will be the same. This is precisely what has been observed in measurements that will be presented in Section V. The reason is that the average output will be the one necessary to keep the system on the control surface, i.e., $\text{LPF}\{b_n\} = \alpha(x)$.

A. Effect of external disturbances and model uncertainties

Model uncertainties and external disturbances of the system are usually represented by a vector $\phi(x,t) \in \mathbb{R}^n$ such that (21) in our case takes the form:

$$\dot{x} = \frac{1}{2}(A_{b_1} + A_{b_0})x + \frac{1}{2}(B_{b_1} + B_{b_0}) + B(x)u + \phi(x,t) \quad (27)$$

where:

$$B(x) = \frac{1}{2}(A_{b_1} - A_{b_0})x + \frac{1}{2}(B_{b_1} - B_{b_0}) \quad (28)$$

and $u = \text{sgn}(\sigma(x))$. As it is well known, disturbances can be decomposed in a matched, $\phi_M(x,t)$, and a mismatched, $\phi_U(x,t)$ component, so that: $\phi(x,t) = \phi_M(x,t) + \phi_U(x,t)$. The matched component lies inside the space spanned by the column vectors of matrix $B(x)$, whereas the mismatched component is defined as the component lying on the complementary vector space, i.e., the null space of the columns of $B(x)$. This means that there is a function $u_M(x,t) \in \mathbb{R}$ such that $\phi_M(x,t) = B(x)u_M(x,t)$. Taking this into account, and assuming that the sliding conditions are still met, equations (25) and (26) are modified as:

$$\alpha(x,t) = -\frac{c^T(A_{b_0}x + B_{b_0} + \phi_U(x,t))}{c^T(A_{b_1} - A_{b_0})x + c^T(B_{b_1} - B_{b_0})} - \frac{u_M(x,t)}{2} \quad (29)$$

and

$$\dot{x} = \alpha(x)\left(A_{b_1}x + B_{b_1}\right) + (1-\alpha(x))\left(A_{b_0}x + B_{b_0}\right) + \phi_U(x,t) \quad (30)$$

This means that, within some limits (it must be $\alpha(x,t) \in [0,1]$), the control method will be able to handle successfully some disturbances and parameter uncertainties. The matched component is cancelled out directly by the equivalent control. The mismatched component, though, generates changes in the global trajectory of the system within the control surface as well as in the equivalent control, as it can be seen in equation (30).

B. Asymptotic control values

As it has been previously shown, and as it is usual in sliding mode control, there are two phases in this kind of controls. In the first phase, the control saturates and therefore applies a constant sequence of either BIT0 or BIT1 symbols. In the second phase, the system is within the control surface and the necessary average control to keep it there is the one obtained in (25). The time evolution of the state variables is then governed by (26). At this point we are interested in the stationary state that will be reached in the long term once we are within the control surface.

If there is a final equilibrium point within the sliding set on the control surface, then there is an equivalent control (b) that can be applied to the average system:

$$\dot{x} = \left(bA_{b_1} + (1-b)A_{b_0}\right)x + bB_{b_1} + (1-b)B_{b_0} \quad (31)$$

to reach asymptotically the desired charge value, i.e., $c^T x_{\text{eq}}(b) - Q_{\text{target}} = 0$. A function $x_{\text{eq}}(b) : [0,1] \to \mathbb{R}^n$ may be defined as the asymptotic equilibrium point of an average system, (31) on which an equivalent control b is applied:

$$x_{\text{eq}}(b) := -\left(bA_{b1} + (1-b)A_{b0}\right)^{-1}\left(bB_{b1} + (1-b)B_{b0}\right) \quad (32)$$

It must be noted that from Assumption 1 matrix $(bA_{b1} + (1-b)A_{b0})$ is stable and invertible. Now, given an asymptotic value of the bitstream average, b, which is an equivalent control signal, the Q_{target} must be such that:

$$Q_{\text{target}}(b) = c^T x_{\text{eq}}(b) \quad (33)$$

Assuming now that the conditions for the inverse function theorem are fulfilled, it is possible to obtain the inverse function: $b = Q_{\text{target}}^{-1}(Q_{th})$, where the average bitstream is obtained as a function of the charge threshold, Q_{th}, or total net charge.

Finally, it must be pointed out that under some conditions we have that $x_{\text{eq}}(b) \in \Omega$, i.e., the attractive sliding region within the control surface, as defined in (20):

Lemma 1: If there is a $b \in (0,1)$ such that $x_{\text{eq}}(b) \in \mathcal{S}$, and $c^T(A_{b_1} - A_{b_0})x_{\text{eq}}(b) < c^T(B_{b_0} - B_{b_1})$, then $x_{\text{eq}}(b) \in \Omega \neq \emptyset$.

Proof. It will be $x_{\text{eq}}(b) \in \Omega$ if and only if $x_{\text{eq}}(b) \in \mathcal{S}, c^T A_{b_1} x_{\text{eq}}(b) < -c^T B_{b_1}$ and $c^T A_{b_0} x_{\text{eq}}(b) > -c^T B_{b_0}$. This obviously means that

$$\begin{aligned} \xi^- &:= c^T A_{b_1} x_{\text{eq}}(b) + c^T B_{b_1} < 0 \\ \xi^+ &:= c^T A_{b_0} x_{\text{eq}}(b) + c^T B_{b_0} > 0 \end{aligned} \quad (34)$$

which means that there must be a $\lambda \in (0,1)$ such that $\lambda\xi^- + (1-\lambda)\xi^+ = 0$. But this number λ is precisely b since:

$$\begin{aligned} b\left[c^T A_{b_1} x_{\text{eq}}(b) + c^T B_{b_1}\right] + \\ +(1-b)\left[c^T A_{b_0} x_{\text{eq}}(b) + c^T B_{b_0}\right] = \\ = c^T\left[bA_{b_1} + (1-b)A_{b_0}\right]x_{\text{eq}}(b) + \\ +c^T\left[bB_{b_1} + (1-b)B_{b_0}\right] = 0 \end{aligned} \quad (35)$$

Finally since from the initial hypothesis in the Lemma $c^T(A_{b_1} - A_{b_0})x_{\text{eq}}(b) < c^T(B_{b_0} - B_{b_1})$, we have that $\xi^- < \xi^+$.

□

Figure 3. Top-view photograph and vertical cross section of device used for the experiment set I.

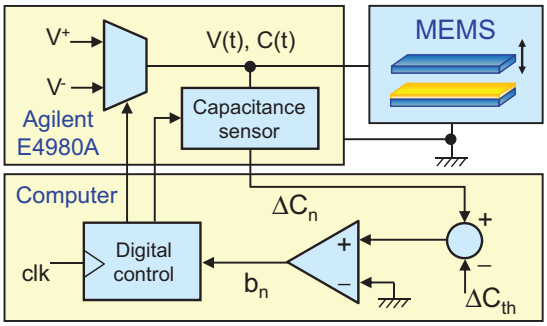

Figure 4. Experimental set-up. The E4980A impedance analyzer is used to sample the capacitance of the device while applying a certain actuation voltage (V^+ or V^-).

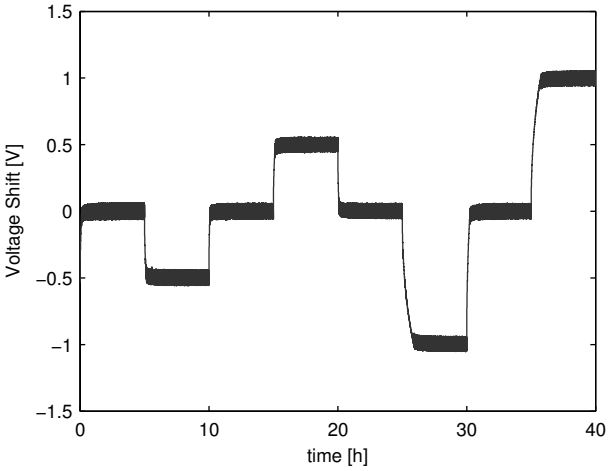

Figure 5. Voltage shift as a function of time for the experiment set I: a second order sigma-delta control of charge with $V^+ = -V^- = 5V$ and $\delta = 0.2, T_S = 2.5s$. The reaching phase segments correspond to the those parts of the plot on which a thin line is apparent, whereas those segments on which the line seems to be wider correspond to the fast switching regime.

It must be noted that in case of a time-invariant system, i.e., $A_{b_0} = A_{b_1}$, condition $c^T(A_{b_1} - A_{b_0})x_{\text{eq}}(b) < c^T(B_{b_0} - B_{b_1})$ is automatically fulfilled.

C. Stability using the dielectric charging models

The dielectric charging models used in [12], [13], [19] behave very well since matrices A_0 and A_1 are diagonal. This implies that assumption 1 is accomplished with any positive diagonal matrix. If we now apply Theorem 2 in [25] to these models we may state the following: if there are Δ and $b \in (0,1)$ such that $c^T x_{\text{eq}}(b) - \Delta = 0$ and $(A_{b_0} - A_{b_1})x_{\text{eq}}(b) + (B_{b_0} - B_{b_1}) > 0$ then $x_{\text{eq}}(b)$ is asymptotically stable.

V. Experimental results

The objective of this section is to present experimental results showing the behavior of the sigma-delta charge control methods analyzed from the perspective of sliding mode controllers. To this effect two sets of experiments have been carried out using two MEMS made with PolyMUMPS technology. Each device is a polysilicon plate suspended over a 2.75μm air gap and a silicon nitride layer of 0.6μm, deposited on top of the silicon wafer, see Figure 3. The first device, used in experiment set I, has an area of 360 x 360 μm^2 and a pull-in voltage of 24V, whereas the second one has an area of $500 \times 500\mu$m^2 and a pull-in voltage of 14V. The application of these control techniques to the operation of non-MEMS devices such as organic FETs or flash memories is an open problem.

The control method is implemented using an Agilent E4980A impedance analyzer that has been programmed to carry out the control method: capacitance measurement at the desired level of voltage. A schematic of the measurement set-up can be seen in Figure 4.

A. Experiment set I: reaching phase of the target surface

The purpose of this experiment is to illustrate the reaching phase of the charge control and the beginning of the fast switching regime (sliding mode). To this effect, a first experiment has been made on which a second order control of charge is used to set different levels of target charge as a function of time: $V_{\text{sh}} = \{0V, -0.5V, 0V, +0.5V, 0V, -1V, 0V, +1V\}$. Each step lasts for 5 hours, and between any two different from zero segments there is a middle segment on which the device is reset to a zero voltage shift. Since the quasi-differential capacitance measurement is being continuously made at each sampling period, it is possible to monitor the evolution of the voltage shift during the experiment, see Figure 5.

The zero target intervals have been inserted to ensure that when changing the voltage shift from a zero target charge to a different target charge, the initial condition of the device is approximately the same. This allows us to superimpose the reaching phase for each of the four different target voltage shifts: $\pm 0.5V, \pm 1V$, see Figure 6. As it can be observed, the device is initially discharged, around $V_{\text{sh}} = 0$ and the common part of the trajectories for positive voltage shifts: $+0.5V$ and $+1V$ (reaching phase) cannot be distinguished. The same happens for the negative target charges (although there is a slight difference for the target curve reaching the $-0.5V$ target voltage shift).

In Figure 6 it is also possible to observe a small difference in the dynamics of positive and negative charge, since the necessary time to reach $+1V$ or $-1V$ is slightly different (around 10 minutes).

It must be noted that once the charge control reaches the desired control surface, total charge constant and equal to Q_{target},

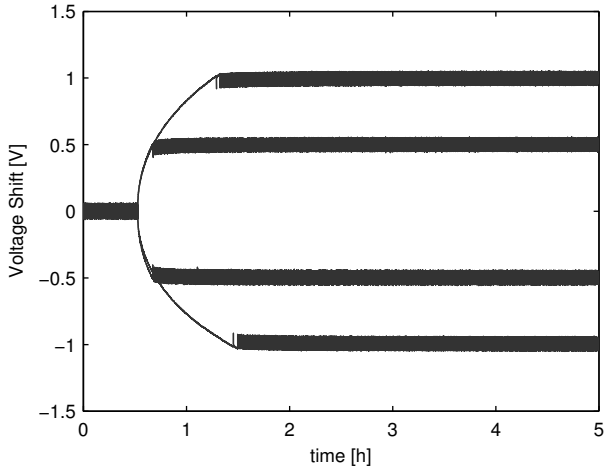

Figure 6. Superimposition of the reaching phase time segments for each target voltage shift set during experiment set I in Figure 5. In the reaching phase of experiments with target voltage shift = $+0.5V$ and $+1V$, only BIT0 symbols where applied (increase of charge). In the reaching phase of $-0.5V$ and $-1V$ target voltage shifts, only BIT1 symbols were applied (decrease of charge).

there is continuous switching of the symbols being applied. This is what in fact will generate the typical quantization noise shaping characteristic of sigma-delta modulators. The same happens in the case of thermal sigma-delta modulation, [26]. This corresponds to what in sliding mode control literature is called chattering. The amount of maximum switching per unit time is limited in this case by the sigma-delta frequency. In the case of sigma-delta controls of charge it can be very low (in our case $T_S = 2.5s$), while keeping quite constant the amount of total charge.

B. Experiment set II: sliding mode analysis of the fast switching regime within the target surface

The second experiment consists on comparing the bitstream obtained in a measurement, with results of discrete time simulations, and also with the sliding analysis of the controllers presented in this work. To this effect, an experiment on a device from which a charge model fitting has been obtained, [19], is used.

In this experiment three different target voltage shifts are applied (+0.5V, -0.75V and 0V) to a device using a first-order sigma-delta controller, see Figure 7. Each target voltage shift is applied for 48 hours. The reason for these long times is that the stabilization times associated with the bitstream are very long, since the time constants of the dynamical charging model are very large (see Table I). As a second step of this experiment the same sequence of voltage shifts with the same timing has been enforced on the device, using in this case a second order controller. In both cases, the sampling time is $T_S = 2.5s, \delta = 0.2$ and $V^+ = -V^- = 4V$. The voltage shift curve as a function of time is practically identical to the one shown in Figure 7, and therefore it is not shown.

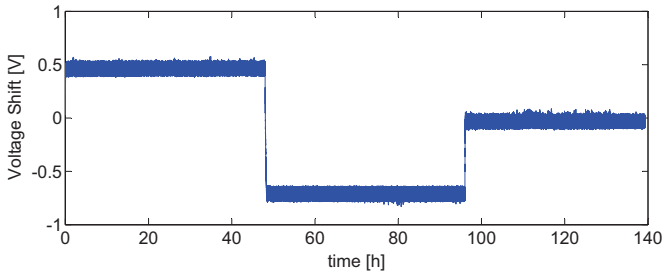

Figure 7. Voltage shift as a function of time for experiment set II. The voltage target shifts are $+0.5V, -0.75V, 0V$. The experiment parameters are $V^+ = -V^- = 4V, \delta = 0.2, T_S = 2.5s$. Each target shift is applied for 48 hours.

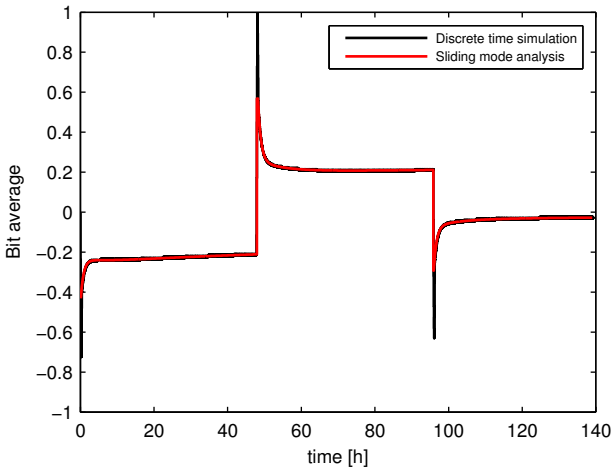

Figure 8. Comparison between the discrete-time simulation corresponding to the experiment of Figure 7, using the model of Table I, with the trajectory of the system obtained by numerically solving equations (25) and (26). As it can be observed both curves cannot be distinguished.

In order to analyze whether the sliding mode approximation may explain the dynamics of the system under control, Figure 8 shows the comparison between the discrete-time simulation of a first-order controller executing the reference experiment, and the time evolution predicted by the sliding mode analysis. The first phase in the sliding mode analysis consists on applying a constant sequence of BIT0 symbols to the device, until the control surface is reached, namely $\sigma = c^T x - Q_{\text{target}} = 0$. Once within the control surface, the system undergoes the sliding motion predicted by equation (26), and produces the average bitstream predicted by (25). At each time the target voltage shift is changed, each 48 hours, another displacement is made in open loop mode (either applying a constant actuation of either BIT0 or BIT1 symbols) until the next control surface is reached. Then the sliding motion is again calculated. As it can be observed in Figure 8 there is a very good matching between the discrete time simulations and the sliding analysis. The difference at the target voltage shift switching instants (each 48 hours) comes from the fact that the average bitstream in the discrete time simulations is obtained by filtering the simulated bitstream.

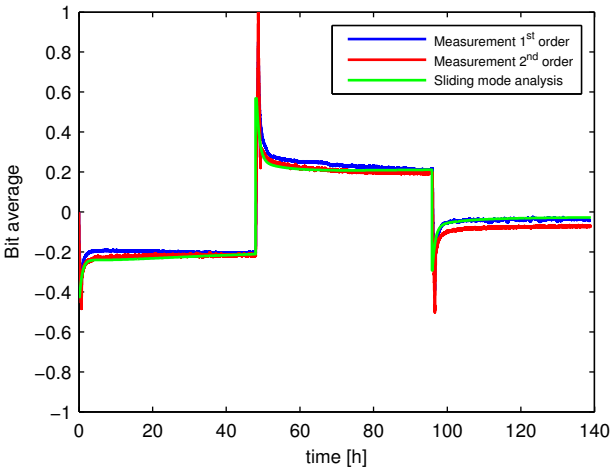

Figure 9. Comparison between the sliding mode analysis shown in Figure 8, with the actual measurements obtained with first and second order sigma-delta modulators.

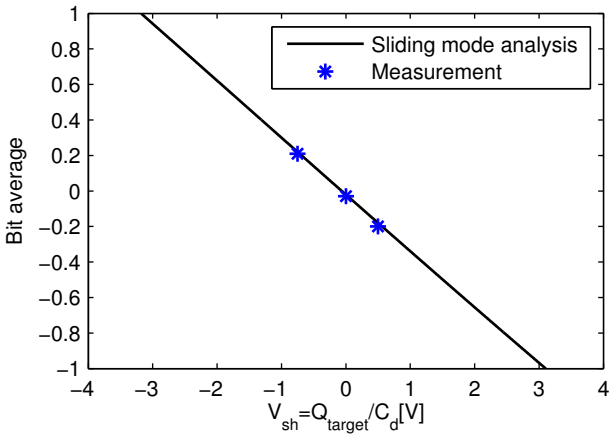

Figure 10. Asymptotic average bitstream $b = Q^{-1}_{\text{target}}(V_{sh})$, for the model of Table I, obtained using expressions (32) and (33). C_d is the capacitance of the dielectric layer and therefore V_{sh} is the voltage shift of the C-V curve of the device. The three points superimposed correspond to the asymptotic bitstream averages obtained in the measurements of Figure 9.

During the time segments of the first phase the system is saturated and this generates a slight overshoot with regard to the average bitstream predicted by the sliding analysis.

Figure 9 shows the comparison between the experimental results obtained with the device in the experiment set II, using both first and second order controllers, and the sliding model analysis proposed in this work. This figure shows an excellent agreement between the discrete time simulations, taking into account all the switching during each control symbol, and the sliding mode analysis.

Finally, Figure 10 shows the asymptotic bitstream values as a function of the target voltage shifts, as predicted by the sliding mode analysis. As it has been mentioned previously, this plot is in fact the inverse function of $Q_{\text{target}}(b)$, as defined

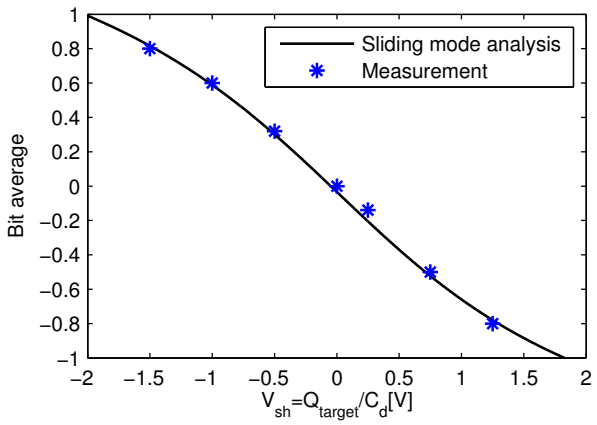

Figure 11. The same analysis as in the case of Figure 10 performed for a different device, [13, Table II], using $V^+ = -V^- = 4V, T_S = 2.5s, \delta = 0.2$. The asymptotic curve predicted by the sliding analysis no longer looks like a straight line.

in (32) and (33). The three asymptotic points obtained in the reference measurements have been superimposed in the figure. It must be noted, that although it looks like an affine function, there may be a non-affine relation between the target charge and the average bitstream, if the charge model parameters are changed. This can be more clearly seen in Figure 11. This figure shows the result of the same asymptotic analysis performed with the device described in [13, Table II]. As it can be seen the bitstream curve no longer looks like a straight line and is basically due to a large disparity in the value of the charging and discharging time constants.

VI. Conclusions

The connection between the sigma-delta dielectric charge controls and sliding mode controllers has been shown. First the average actuation system has been obtained on which the dynamics of the system depends directly on the control sequences, taking into account the voltage switching during the sampling period. This average system is equivalent to the actuation with sigma-delta modulators at infinite sampling frequency. Once, this equivalence has been found, the dynamics of the system is analyzed within the scope of sliding mode controllers. This analysis allows to understand and predict the dynamics of the net dielectric charge under this kind of controls. Specifically it allows to understand the response of the control bitstreams as a function of the hidden state variables of the multiexponential charge model.

References

[1] H. H. Choi, W. H. Lee, and K. Cho, "Bias-stress-induced charge trapping at polymer chain ends of polymer gate-dielectrics in organic transistors," *Advanced Functional Materials*, vol. 22, no. 22, pp. 4833–4839, 2012. [Online]. Available: http://dx.doi.org/10.1002/adfm.201201084

[2] H. H. Choi, M. S. Kang, M. Kim, H. Kim, J. H. Cho, and K. Cho, "Decoupling the bias-stress-induced charge trapping in semiconductors and gate-dielectrics of organic transistors using a double stretched-exponential formula," *Advanced Functional Materials*, vol. 23, no. 6, pp. 690–696, 2013. [Online]. Available: http://dx.doi.org/10.1002/adfm.201201545

[3] J.-M. Lee, I.-T. Cho, J.-H. Lee, and H.-I. Kwon, "Bias-stress-induced stretched-exponential time dependence of threshold voltage shift in ingazno thin film transistors," *Applied Physics Letters*, vol. 93, no. 9, pp. –, 2008. [Online]. Available: http://scitation.aip.org/content/aip/journal/apl/93/9/10.1063/1.2977865

[4] P. Moon, J. Y. Lim, T.-U. Youn, S.-K. Park, and I. Yun, "Field-dependent charge trapping analysis of {ONO} inter-poly dielectrics for {NAND} flash memory applications," *Solid-State Electronics*, vol. 94, no. 0, pp. 51 – 55, 2014. [Online]. Available: http://www.sciencedirect.com/science/article/pii/S0038110114000227

[5] W. Lee, J. Jee, D.-H. Yoo, E.-Y. Lee, J. Bok, Y. Hyung, S. Kim, C.-J. Kang, J.-T. Moon, and Y. Roh, "Leakage current reduction mechanism of oxide–nitride–oxide inter-poly dielectrics through the post plasma oxidation treatment," *Japanese Journal of Applied Physics*, vol. 50, no. 4R, p. 041501, 2011. [Online]. Available: http://stacks.iop.org/1347-4065/50/i=4R/a=041501

[6] S. Lucuszyn (edt.), *Advanced RF MEMS*. Cambridge University Press, 2010.

[7] W. Spengen, "Capacitive RF MEMS switch dielectric charging and reliability: a critical review with recommendations," *Journal of Micromechanics and Microengineering*, vol. 22, 2012.

[8] T. Ikehashi, T. Miyazaki, H. Yamazaki, A. Suzuki, E. Ogawa, S. Miyano, T. Saito, T. Ohguro, T. Miyagi, Y. Sugizaki, N. Otsuka, H. Shibata, and Y. Toyoshima, "An RF MEMS variable capacitor with intelligent bipolar actuation," in *IEEE International Solid-State Circuits Conference (ISSCC 2008)*, Feb 3-7, 2008, pp. 581–583.

[9] U. Zaghloul, G. Papaioannou, F. Coccetti, P. Pons, and R. Plana, "Dielectric charging in silicon nitride films for MEMS capacitive switches: Effect of film thickness and deposition conditions," *Microelectronics Reliability*, vol. 49, pp. 1309–1314, 2009.

[10] G. Rebeiz, *RF MEMS theory, design and technology*. Wiley, 2003.

[11] M. Dominguez-Pumar, D. Lopez, D. Molinero, and J. Pons, "Dielectric charging control for electrostatic mems switches," in *Proc. of SPIE Conf. on Defense, Security and Sensing DSS-2010*, vol. 7679, pp. 1-11, Orlando, 2010.

[12] E. Blokhina, S. Gorreta, D. Lopez, D. Molinero, O. Feely, J. Pons-Nin, and M. Dominguez-Pumar, "Dielectric charge control in electrostatic MEMS positioners / varactors," *IEEE JMEMS*, vol. 21, pp. 559–573, 2012.

[13] S. Gorreta, J. Pons-Nin, E. Blokhina, O. Feely, and M. Dominguez-Pumar, "Delta-sigma control of dielectric charge for contactless capacitive mems," *Microelectromechanical Systems, Journal of*, vol. 23, no. 4, pp. 829–841, Aug 2014.

[14] S. Gorreta, J. Pons-Nin, E. Blokhina, and M. Dominguez, "A second-order delta-sigma control of dielectric charge for contactless capacitive mems," *Microelectromechanical Systems, Journal of*, vol. PP, no. 99, pp. 1–1, 2015.

[15] J. Zhang and W. X. Zheng, "Design of adaptive sliding mode controllers for linear systems via output feedback," *Industrial Electronics, IEEE Transactions on*, vol. 61, no. 7, pp. 3553–3562, July 2014.

[16] S. Qu, X. Xia, and J. Zhang, "Dynamics of discrete-time sliding-mode-control uncertain systems with a disturbance compensator," *Industrial Electronics, IEEE Transactions on*, vol. 61, no. 7, pp. 3502–3510, July 2014.

[17] H. Sira-Ramirez, M. Zribi, and S. Ahmad, "Pulse width modulated control of robotic manipulators," *International Journal of Systems Science*, vol. 24, no. 8, pp. 1423–1437, 1993.

[18] P. Bolzern and W. Spinelli, "Quadratic stabilization of a switched affine system about a nonequilibrium point," in *American Control Conference, 2004. Proceedings of the 2004*, vol. 5, June 2004, pp. 3890–3895 vol.5.

[19] M. Dominguez-Pumar, S. Gorreta, J. Pons-Nin, E. Blokhina, P. Giounanlis, and O. Feely, "Real-time characterization of dielectric charging in contactless capacitive mems," *Analog Integrated Circuits and Signal Processing*, vol. 82, no. 3, pp. 559–569.

[20] N. Cohen and I. Lewkowicz, "A pair of matrices sharing common Lyapunov solutions—A closer look," *Linear Algebra and its Applications*, vol. 360, pp. 83–104, 2003.

[21] V. D and J. N. Tsitsiklis, "Complexity of stability and controllability of elementary hybrid systems," *Automatica*, vol. 35, no. 3, pp. 479 – 489, 1999.

[22] M. Bernardo, C. Budd, A. Champneys, and P. Kowalczyk, *Piecewise-smooth dynamical systems*. Springer, 2008.

[23] J. Gonçalves, A. Megretski, and M. Dahleh, "Global stability of relay feedback systems," *Automatic Control, IEEE Transactions on*, vol. 46, no. 4, pp. 550–562, Apr 2001.

[24] J. Goncalves, A. Megretski, and M. Dahleh, "Global analysis of piecewise linear systems using impact maps and surface lyapunov functions," *Automatic Control, IEEE Transactions on*, vol. 48, no. 12, pp. 2089–2106, Dec 2003.

[25] G. S. Deaecto, J. C. Geromel, F. Garcia, and J. Pomilio, "Switched affine systems control design with application to dc–dc converters," *IET control theory & applications*, vol. 4, no. 7, pp. 1201–1210, 2010.

[26] M. Dominguez-Pumar, V. Jimenez, J. Ricart, L. Kowalski, J. Torres, S. Navarro, J. Romeral, and L. Castañer, "A hot film anemometer for the Martian atmosphere," *Planetary and Space Science*, vol. 56, p. 1169–1179, 2008.